PHYSICAL REVIEW B **95**, 100403(R) (2017)

Nonreciprocity of electrically excited thermal spin signals in CoFeAl-Cu-Py lateral spin valves

Shaojie Hu,[1,2,3,*] Xiaomin Cui,[4] Tatsuya Nomura,[5] Tai Min,[1,2] and Takashi Kimura[3,5,†]

[1]*Center of Spintronics and Quantum System, Xi'an Jiaotong University, No. 28 Xianning West Road Xi'an, Shaanxi 710049, People's Republic of China*

[2]*School of Materials Science and Engineering, Xi'an Jiaotong University, No. 28 Xianning West Road Xi'an, Shaanxi 710049, People's Republic of China*

[3]*Research Center for Quantum Nano-Spin Sciences, Kyushu University, 744 Motooka, Fukuoka 812-8581, Japan*

[4]*Shaanxi Key Laboratory of Condensed Matter Structures and Properties, School of Science, Northwestern Polytechnical University, Xi'an 710072, People's Republic of China*

[5]*Department of Physics, Kyushu University, 744 Motooka, Fukuoka 812-8581, Japan*

(Received 26 September 2016; revised manuscript received 18 February 2017; published 20 March 2017)

Electrical and thermal spin currents excited by an electric current have been systematically investigated in lateral spin valves consisting of CoFeAl and $Ni_{80}Fe_{20}$ (Py) wires bridged by a Cu strip. In the electrical spin signal, the reciprocity between the current and voltage probes was clearly confirmed. However, a significant nonreciprocity was observed in the thermal spin signal. This provides clear evidence that a large spin-dependent Seebeck coefficient is more important than the spin polarization for efficient thermal spin injection and detection. We demonstrate that the spin-dependent Seebeck coefficient can be simply evaluated from the thermal spin signals for two configurations. Our experimental description paves a way for evaluating a small spin-dependent Seebeck coefficient for conventional ferromagnets without using complicated parameters.

DOI: 10.1103/PhysRevB.95.100403

The efficient generation and detection of the spin current is a crucial issue for the application of spintronic devices [1–3]. In addition, the integration of spintronic circuits with conventional semiconductor devices is another important milestone for the practical application of spin devices. Recently, the interplay between the heat and spin has attracted great attention [4–8], while the temperature gradient is found to excite spin current injection from the ferromagnet to nonferromagnet in various bilayer systems based on different mechanisms, such as the so-called spin Seebeck effect in ferromagnetic metals and insulators [9–12], the spin-dependent Seebeck effect in metallic junctions [13–18], the Seebeck spin tunnel effect [19–22], the magnon-driven effect [23,24], and spin heat accumulation [25–27]. Since the heat can be generated by microwave absorption in an open circuit without an electric current [28–31], this approach using heat may open an avenue for simplifying the integration of spin devices.

In metallic ferromagnetic/nonmagnetic (F/N) hybrid structures, the spin-dependent Seebeck effect is one paramount mechanism for thermal spin injection [13,32]. The generation efficiency of thermally excited spin current is dominated by the spin-dependent Seebeck coefficient $S_S = S_\uparrow - S_\downarrow$, which is the difference in a Seebeck coefficient for the up-spin and down-spin electrons in the ferromagnet. Therefore, the determination of S_S is indispensable to quantify thermally excited spin current as well as the optimization of the thermospin properties of ferromagnets [33]. However, the quantitative estimation of S_S is still a difficult problem to solve for a conventional ferromagnets because the tiny spin asymmetry of the Seebeck coefficient results in a poor generation efficiency of the spin current. Moreover, the spin-related signals are smeared out by spurious signals induced by the intrinsic thermoelectric effects in the ferromagnet, such as the anomalous Nernst effect and the anisotropic magneto-Seebeck effect, especially at room temperature [34–38]. The exploration of appropriate device structures and excellent materials could be an approach to assist the estimation of S_S of conventional ferromagnets.

Recently, demonstrations of the spin-dependent Seebeck effect have been reported by extending the nonlocal spin valve measurement in a lateral spin valve structure combined with the second harmonic detection technique. This approach not only evaluates the spin transport properties but also extracts the thermospin effect from the spurious thermoelectric effect [13,17]. Additionally, we demonstrate that CoFeAl has excellent thermal spin injection efficiency because of its favorable band structures [16,39]. However, the large thermal spin signal is not only contributed by the excellent spin-dependent Seebeck coefficient but also by the large spin polarization of CoFeAl. It is more effective to show the large spin-dependent Seebeck coefficient of CoFeAl by a persuasive experiment. In this Rapid Communication, by utilizing the excellent electrical and thermal spin injection properties of CoFeAl, we show that the thermospin property in conventional ferromagnetic metals with small spin-dependent Seebeck coefficients can be precisely evaluated.

A lateral spin valve (LSV) consisting of CoFeAl (CFA) and NiFe (Py) wires bridged by a Cu strip was fabricated on a SiO_2/Si substrate by multistep electron-beam lithography and lift-off techniques. Figure 1(a) shows the scanning electron microscopy (SEM) image and the schematic illustration of the present lateral spin valve, where the center-center distance between the two ferromagnetic wires L is 350 nm. Py and CoFeAl were deposited by an electron-beam evaporator under an ultrahigh vacuum of 1.5×10^{-7} Pa. The thicknesses of the two ferromagnetic wires are 30 nm. Here, the CoFeAl wire was connected to the large contact pads at the wire end, although the NiFe wire has flat ends. This leads to the difference in the

*shaojiehu@mail.xjtu.edu.cn
†t-kimu@phys.kyushu-u.ac.jp

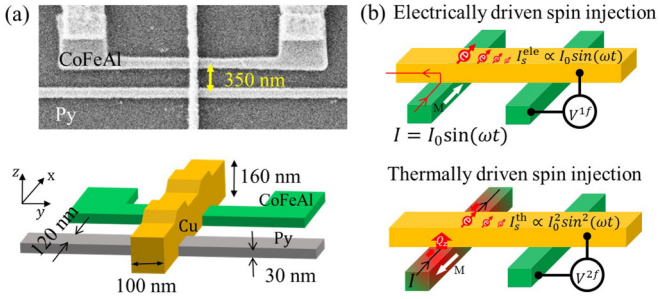

FIG. 1. (a) SEM image and the schematic illustration of the present lateral spin valve. (b) Measurement configuration for the electrically and thermally driven spin injections. In electrically driven spin injection, when the bias current flows through the F/N junction, the generated spin current is detected by measuring the first harmonic responding voltage. In thermally driven spin injection, when the bias current flows through the ferromagnetic wire without passing through the junction, the spin current generated by the temperature gradient due to Joule heating is detected by measuring the second harmonic responding voltage.

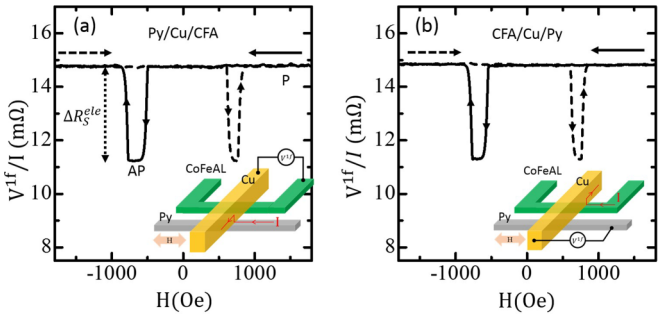

FIG. 2. Electrically driven nonlocal spin valve curves for the device with 350 nm interval distance together with the measurement probe configuration. (a) Bias current flows through the Py/Cu junction, and the electrically driven spin current will be detected by the first harmonic voltage with sweeping magnetic field at the CoFeAl/Cu(CFA/Cu) junction. The spin signal ΔR_S^{ele} is defined as the normalized value of the voltage difference between the parallel and antiparallel by the injection current. (b) The CoFeAl/Cu junction works as the spin injector and the Py/Cu junction works as the spin current detector. The dashed and solid arrows correspond to the directions of the sweeping field.

switching field, which enables us to control the magnetization configuration [parallel (P) and antiparallel (AP) alignments] by sweeping the magnetic field. The 160-nm-thick Cu channel was deposited by thermal evaporation under a base pressure of 10^{-6} Pa. Before the deposition of Cu, both the surfaces of the CoFeAl and Py wires were well cleaned by an Ar^+ ion beam with a low acceleration voltage. The lateral dimensions for the CoFeAl/Cu and Py/Cu junctions are 120×100 nm^2. The interface transparency was confirmed by a four-terminal contact-resistance measurement.

As shown in Fig. 1(b), for the detection of the electrically driven spin current, a small ac bias current $[I_0 \sin(\omega t)]$ was applied across the F/N junction. Since the influence of the Joule heating effect is negligibly small because of the low bias current density, the electrical spin current shows the first harmonic frequency response. On the other hand, when the bias current in the F wire is very large, local heating will be produced in the two segments of the F wire, as shown in Fig. 1(b). In this situation, owing to the high thermal conductivity of the Cu strip, which is much larger than that of the substrate, most of the produced heat current flows into the Cu strip across the F/N junction, resulting in thermal spin injection. Since the thermally excited spin current due to the electric current is proportional to the current square $[I_0 \sin(\omega t)^2]$, we can extract the thermal contribution in the electrical signal by detecting the second harmonic voltage.

First, the electrically excited spin injection and detection properties are evaluated by conventional nonlocal spin valve measurements with the probe configuration shown in the inset of Fig. 2(a). We measured the nonlocal spin signal (ΔR_S) which is the voltage change between the P and AP states normalized by the bias current. Here, we evaluate ΔR_S for two configurations, as schematically shown in the insets of Figs. 2(a) and 2(b). One is the CoFeAl injector and Py detector (configuration A). The other one is the Py injector and the CoFeAl detector (configuration B). Figures 2(a) and 2(b) show the field dependences of the nonlocal spin valve curves for configurations A and B, respectively. The spin signals (ΔR_S^{ele}) for configuration A are 3.53 ± 0.02 mΩ, which is almost the same as that for configuration B. We additionally studied the other three LSVs consisting of CoFeAl and Py wires with different intervals L and confirmed a similar relationship.

These probe configuration dependences can be understood as follows. According to the one-dimensional spin diffusion model [40,41], the electrical spin signal in the lateral spin valve consisting of two different kinds of ferromagnetic wires could be expressed by the following equation [42–44],

$$\Delta R_S^{ele} = \frac{P_I P_D R_{FI} R_{FD} R_N}{[2R_{FI}R_{FD} + R_N(R_{FI}+R_{FD})][\cosh(L/\lambda_N)+\sinh(L/\lambda_N)] + R_N^2 \sinh(L/\lambda_N)}, \quad (1)$$

where P_I and P_D are the spin polarizations for the injector and detector. λ_N is the spin diffusion length for the nonferromagnet. R_{FI}, R_{FD}, and R_N are the spin resistances for the injector, detector and nonferromagnet, respectively. The spin resistance is defined as $2\rho\lambda/[A(1-P^2)]$, where P, ρ, and λ are the spin polarization, resistivity, and spin diffusion length, respectively. For a nonmagnet, P is zero and A is given by the area of the effective cross section for the spin current. For a ferromagnet, since the spin diffusion length is known to be quite short, the effective cross section should be given by the area of the F/N junction.

Figure 3 shows the spin signals for the CFA-Cu-Py LSVs as a function of interval distance L. For comparisons, the spin signals for the Py/Cu/Py and CFA/Cu/CFA were also plotted

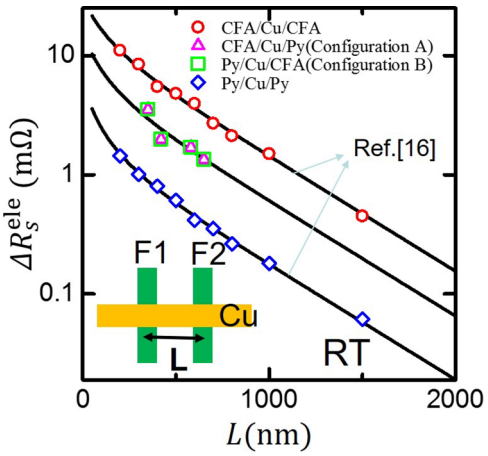

FIG. 3. Interval distance dependence of the electrical spin signals in different lateral spin valves. CFA-Cu-Py and Py-Cu-CFA correspond to the reversed injector and detector for the same lateral spin valve containing two kinds of ferromagnets CFA and Py.

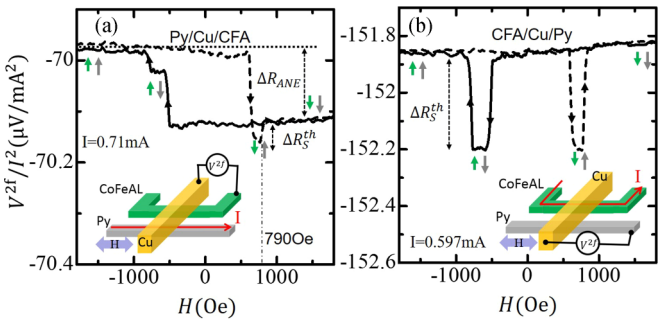

FIG. 4. Nonlocal spin curve for thermally driven spin injection together with the schematic illustration of the measurement probe configurations. The two solid arrows represent the direction of the magnetization for the two ferromagnets. (a) Thermally induced nonlocal signals with the Py wire as an injector and the CoFeAl wire as a detector. We refer to this configuration as "configuration A." Here, the bias current in the Py wire is 0.71 mA. (a) Thermally induced nonlocal signals with the CoFeAl wire as an injector and the Py wire as a detector. We refer to this configuration as "configuration B." Here, the bias current is 0.60 mA.

in the same graph. Here, it should be noted that all results are well fitted by Eq. (1) with the parameters of $P_{\mathrm{CFA}} = 0.62$, $P_{\mathrm{Py}} = 0.36$, $\lambda_{\mathrm{CFA}} = \lambda_{\mathrm{Py}} = 2$ nm, and $\lambda_{\mathrm{Cu}} = 450$ nm at room temperature. This indicates the validity of the one-dimensional spin diffusion model and high reproducibility of our lateral spin valves. Using Eq. (1) and the data on the CFA/Cu/Py sample in both configurations A and B, we obtained almost the same value of the spin signal, which indicates a reciprocal relationship between the spin injector and detector in the nonlocal spin valve signal. Slight differences between the two configurations observed in the experiments may be caused by extrinsic contributions, such as an inhomogeneous current distribution and higher-order effects [45–48].

We then evaluated the thermally excited spin current in the CFA/Cu/Py LSVs. Figures 4(a) and 4(b) show the nonlocal spin valve signals under thermal spin injection with the probe configurations shown in the insets of each figure. Here, the current flows only in the ferromagnetic wire and did not flow across the interface between F and N, meaning an electrically excited spin current does not exist in the Cu wire. In Fig. 4(a), we can see a quite unconventional feature in the field dependence of the nonlocal signal. The field dependence of the voltage change is asymmetric with respect to $H = 0$. This asymmetric feature can be explained by the anomalous Nernst effect in the ferromagnetic voltage probe [38,49,50]. Owing to the relatively large thermal conductivity in the Cu wire, the injected heat current diffuses in the Cu wire isotropically and reaches the detecting junction. A finite heat current diffuses into the CFA detector across the CFA/Cu junction. This induces a measurable anomalous Nernst voltage in between the CFA and Cu voltage probes. The field dependence of the voltage change due to the Nernst effect should show odd functions, although the spin signal shows an even function. Therefore, we can clearly separate the thermally excited spin signal and extrinsic Nernst effect. The obtained thermal spin signal ΔR_S^{th} is approximately 0.04 μV/mA^2 using the Py injector and CoFeAl detector shown in Fig. 4(a). On the other hand, as can be seen in Fig. 4(b), we observe a clearer spin signal with a magnitude of 0.34 μV/mA^2 with a relatively small asymmetric field dependence. This is because the CoFeAl wire has a large spin-dependent Seebeck coefficient and the flat-end shape of the Py wire suppressed the heat propagation from the Cu wire [38]. Thus, in thermal spin signals, nonreciprocal relations were clearly observed.

To understand these unique characteristics observed in the thermal spin signals, we analyze the experimental results more quantitatively. By adapting the one-dimensional spin diffusion model in a conventional lateral spin valve structure, we can derive the thermally driven spin voltage as follows [13,16],

$$\Delta V_{\mathrm{S}}^{\mathrm{th}} = \frac{P_{\mathrm{D}} R_{\mathrm{FD}} R_{\mathrm{N}} \lambda_{\mathrm{FI}} S_S \nabla T_{\mathrm{I}}}{[2R_{\mathrm{FI}} R_{\mathrm{FD}} + R_{\mathrm{N}}(R_{\mathrm{FI}} + R_{\mathrm{FD}})][\cosh(L/\lambda_{\mathrm{N}}) + \sinh(L/\lambda_{\mathrm{N}})] + R_N^2 \sinh(L/\lambda_{\mathrm{N}})}, \tag{2}$$

where ∇T_{I} is the temperature gradient around the interface of the ferromagnetic injector. Most of the parameters except for S_S have been obtained from the nonlocal electrical spin injection experiments describe above. Regarding ∇T_{I}, the heat power due to Joule heating is proportional to the current square, and we can assume that $\nabla T_{\mathrm{I}} = \gamma \rho I^2$. Here, γ is a constant parameter which mainly depends on the thermal conductivity of the ferromagnet and can be estimated from the numerical calculation based on COMSOL [15,16,33].

We performed similar measurements for the other three LSVs with different L and obtained a similar nonreciprocal relationship. Figure 5 shows the thermally excited spin signal

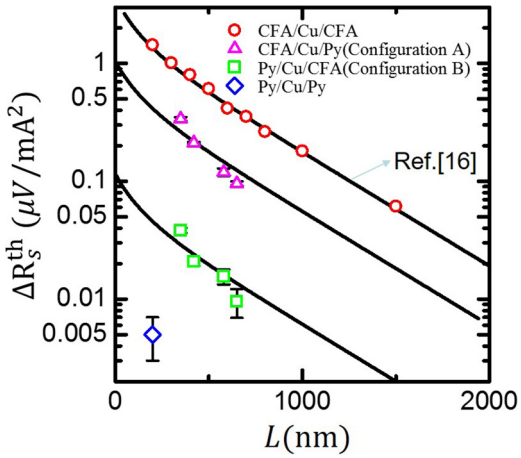

FIG. 5. Interval distance dependence of the thermal spin signals for various types of lateral spin valves.

as a function of the interval distance L for various types of lateral spin valves. It should be noted that all results are well reproduced by Eq. (2) with the same material parameters. Especially, the spin diffusion lengths for the Cu in all LSVs are the same value of 450 nm as that in Fig. 3 even under thermal spin injection. This indicates that the temperature change of the Cu channel is negligibly small because of its large heat capacity. Since the physical parameters in Eq. (2) do not change when interchanging the probe configuration, we can simplify Eq. (2) by introducing the ratio η of the thermally excited spin signals between two configurations as follows,

$$\eta = \frac{\Delta R_{\mathrm{SPy}}^{\mathrm{th}}}{\Delta R_{\mathrm{SCFA}}^{\mathrm{th}}} = \frac{S_S^{\mathrm{Py}}}{S_S^{\mathrm{CFA}}} \frac{\gamma_{\mathrm{Py}}}{\gamma_{\mathrm{CFA}}} \frac{P_{\mathrm{CFA}}/\left(1-P_{\mathrm{CFA}}^2\right)}{P_{\mathrm{Py}}/\left(1-P_{\mathrm{Py}}^2\right)}. \quad (3)$$

Here, most of the experimental parameters were eliminated and the remaining parameters are only P, S_S, and γ. By assuming a thermal conductivity of 46.4 $\mathrm{W\,m^{-1}\,K^{-1}}$ for Py, 29.8 $\mathrm{W\,m^{-1}\,K^{-1}}$ for CFA, 400 $\mathrm{W\,m^{-1}\,K^{-1}}$ for Cu, 1.3 $\mathrm{W\,m^{-1}\,K^{-1}}$ for SiO_2, and 1.4 $\mathrm{W\,m^{-1}\,K^{-1}}$ for Si, we obtained $\gamma_{\mathrm{CFA}}/\gamma_{\mathrm{Py}} = 1.1$. Moreover, the final part in Eq. (3) corresponding to the ratio of $P^2/(1-P^2)$ is 2.4. Therefore, we obtain $S_{\mathrm{Py}}/S_{\mathrm{CFA}}$ as 0.043. From these values, we can estimate the spin-dependent Seebeck coefficient for Py as -2.86 μV/K, and this value is in the same range with previous reports [33]. However, it is 25 times smaller than the value for CFA, providing clear evidence that the large thermal spin signals in the CFA/Cu/CFA LSVs originate from the large thermal spin-dependent Seebeck coefficient for the CFA. Moreover, it also indicates that we can estimate S_S, which is the key experimental factor for thermal spin injection, without using complicated experimental parameters.

In summary, we have investigated the transport properties of the electrically and thermally excited spin currents in CFA-Cu-Py lateral spin valves. Although the electrical spin signal showed a clear reciprocal relationship between the current and voltage probes, a significant nonreciprocity was observed in the thermal spin signals. We showed that both results are quantitatively understood by the one-dimensional spin diffusion model. These results provide clear evidence that a large thermal spin signal was mainly contributed by the large spin-dependent Seebeck coefficient of the CFA. In addition, we demonstrated that the spin-dependent Seebeck coefficient can be simply evaluated from the ratio of thermal spin signals between two configurations. This approach provides a quantitative estimation of a small spin-dependent Seebeck coefficient without using complex experimental parameters.

This work is partially supported by a Grant-in-Aid for Scientific Research on Innovative Area, "Nano Spin Conversion Science" (26103002) and that for Scientific Research(S)(25220605). This work is also partially supported by National Natural Science Foundation for Distinguished Young Scholar of China (Grant No.51601139) and National Key Research Program of China (2016YFA0300702).

[1] S. Maekawa, S. O. Valenzuela, E. Saitoh, and T. Kimura, *Spin Current* (Oxford University Press, Oxford, UK, 2012).
[2] S. R. Bakaul, S. Hu, and T. Kimura, Appl. Phys. A **111**, 355 (2012).
[3] R. L. Stamps, S. Breitkreutz, J. Åkerman, A. V. Chumak, Y. Otani, G. E. W. Bauer, J.-U. Thiele, M. Bowen, S. A. Majetich, M. Kläui, I. L. Prejbeanu, B. Dieny, N. M. Dempsey, and B. Hillebrands, J. Phys. D: Appl. Phys. **47**, 333001 (2014).
[4] M. Johnson and R. H. Silsbee, Phys. Rev. B **35**, 4959 (1987).
[5] L. Gravier, A. Fábián, A. Rudolf, A. Cachin, J.-E. Wegrowe, and J.-P. Ansermet, J. Magn. Magn. Mater. **271**, 153 (2004).
[6] G. E. W. Bauer, E. Saitoh, and B. J. van Wees, Nat. Mater. **11**, 391 (2012).
[7] S. R. Boona, R. C. Myers, and J. P. Heremans, Energy Environ. Sci. **7**, 885 (2014).
[8] X. Jia, K. Xia, and G. E. W. Bauer, Phys. Rev. Lett. **107**, 176603 (2011).
[9] K. Uchida, S. Takahashi, K. Harii, J. Ieda, W. Koshibae, K. Ando, S. Maekawa, and E. Saitoh, Nature (London) **455**, 778 (2008).
[10] J. Sinova, Nat. Mater. **9**, 880 (2010).
[11] K. I. Uchida, H. Adachi, T. Ota, H. Nakayama, S. Maekawa, and E. Saitoh, Appl. Phys. Lett. **97**, 172505 (2010).
[12] C. M. Jaworski, J. Yang, S. Mack, D. D. Awschalom, R. C. Myers, and J. P. Heremans, Phys. Rev. Lett. **106**, 186601 (2011).
[13] A. Slachter, F. L. Bakker, J.-P. Adam, and B. J. van Wees, Nat. Phys. **6**, 879 (2010).
[14] M. Erekhinsky, F. Casanova, I. K. Schuller, and A. Sharoni, Appl. Phys. Lett. **100**, 212401 (2012).
[15] S. R. Bakaul, S. Hu, and T. Kimura, Phys. Rev. B **88**, 184407 (2013).
[16] S. Hu, H. Itoh, and T. Kimura, NPG Asia Mater. **6**, e127 (2014).
[17] K. Yamasaki, S. Oki, S. Yamada, T. Kanashima, and K. Hamaya, Appl. Phys. Express **8**, 043003 (2015).
[18] A. Hojem, D. Wesenberg, and B. L. Zink, Phys. Rev. B **94**, 024426 (2016).
[19] J.-C. Le Breton, S. Sharma, H. Saito, S. Yuasa, and R. Jansen, Nature (London) **475**, 82 (2011).

[20] N. Liebing, S. Serrano-Guisan, K. Rott, G. Reiss, J. Langer, B. Ocker, and H. W. Schumacher, Phys. Rev. Lett. **107**, 177201 (2011).
[21] M. Misiorny and J. Barnaś, Phys. Rev. B **89**, 235438 (2014).
[22] K.-R. Jeon, H. Saito, S. Yuasa, and R. Jansen, Phys. Rev. B **92**, 054403 (2015).
[23] J. Xiao, G. E. W. Bauer, K.-c. Uchida, E. Saitoh, and S. Maekawa, Phys. Rev. B **81**, 214418 (2010).
[24] S. M. Rezende, R. L. Rodríguez-Suárez, R. O. Cunha, A. R. Rodrigues, F. L. A. Machado, G. A. Fonseca Guerra, J. C. Lopez Ortiz, and A. Azevedo, Phys. Rev. B **89**, 014416 (2014).
[25] T. T. Heikkilä, M. Hatami, and G. E. W. Bauer, Phys. Rev. B **81**, 100408 (2010).
[26] F. K. Dejene, J. Flipse, G. E. W. Bauer, and B. J. van Wees, Nat. Phys. **9**, 636 (2013).
[27] I. J. Vera-Marun, B. J. van Wees, and R. Jansen, Phys. Rev. Lett. **112**, 056602 (2014).
[28] F. L. Bakker, J. Flipse, A. Slachter, D. Wagenaar, and B. J. van Wees, Phys. Rev. Lett. **108**, 167602 (2012).
[29] H. Schultheiss, J. E. Pearson, S. D. Bader, and A. Hoffmann, Phys. Rev. Lett. **109**, 237204 (2012).
[30] N. Kuhlmann, C. Swoboda, A. Vogel, T. Matsuyama, and G. Meier, Phys. Rev. B **87**, 104409 (2013).
[31] K. Yamanoi, Y. Yokotani, and T. Kimura, Appl. Phys. Lett. **107**, 182410 (2015).
[32] H.-H. Fu, D.-D. Wu, Z.-q. Zhang, and L. Gu, Sci. Rep. **5**, 10547 (2015).
[33] F. K. Dejene, J. Flipse, and B. van Wees, Phys. Rev. B **86**, 024436 (2012).
[34] A. Slachter, F. L. Bakker, and B. J. van Wees, Phys. Rev. B **84**, 020412 (2011).
[35] S. Y. Huang, W. G. Wang, S. F. Lee, J. Kwo, and C. L. Chien, Phys. Rev. Lett. **107**, 216604 (2011).
[36] A. D. Avery, M. R. Pufall, and B. L. Zink, Phys. Rev. Lett. **109**, 196602 (2012).
[37] C. T. Bui and F. Rivadulla, Phys. Rev. B **90**, 100403(R) (2014).
[38] S. Hu and T. Kimura, Phys. Rev. B **87**, 014424 (2013).
[39] S. Hu and T. Kimura, Phys. Rev. B **90**, 134412 (2014).
[40] M. Johnson and R. H. Silsbee, Phys. Rev. Lett. **55**, 1790 (1985).
[41] T. Valet and A. Fert, Phys. Rev. B **48**, 7099 (1993).
[42] S. Takahashi and S. Maekawa, Phys. Rev. B **67**, 052409 (2003).
[43] T. Kimura, J. Hamrle, and Y. Otani, Phys. Rev. B **72**, 014461 (2005).
[44] S. Nonoguchi, T. Nomura, and T. Kimura, Appl. Phys. Lett. **100**, 132401 (2012).
[45] J. Hamrle, T. Kimura, Y. Otani, K. Tsukagoshi, and Y. Aoyagi, Phys. Rev. B **71**, 094402 (2005).
[46] J. Flipse, F. L. Bakker, A. Slachter, F. K. Dejene, and B. J. van Wees, Nat. Nanotechnol. **7**, 166 (2012).
[47] M. Johnson and R. Silsbee, Phys. Rev. B **76**, 153107 (2007).
[48] F. Bakker, A. Slachter, J.-P. Adam, and B. van Wees, Phys. Rev. Lett. **105**, 136601 (2010).
[49] A. Slachter, F. L. Bakker, and B. J. van Wees, Phys. Rev. B **84**, 174408 (2011).
[50] T. Miyasato, N. Abe, T. Fujii, A. Asamitsu, S. Onoda, Y. Onose, N. Nagaosa, and Y. Tokura, Phys. Rev. Lett. **99**, 086602 (2007).